I.P.N. - 91406 ORSAY CEDEX

institut de physique nucléaire CNRS - IN2P3 UNIVERSITÉ PARIS - SUD

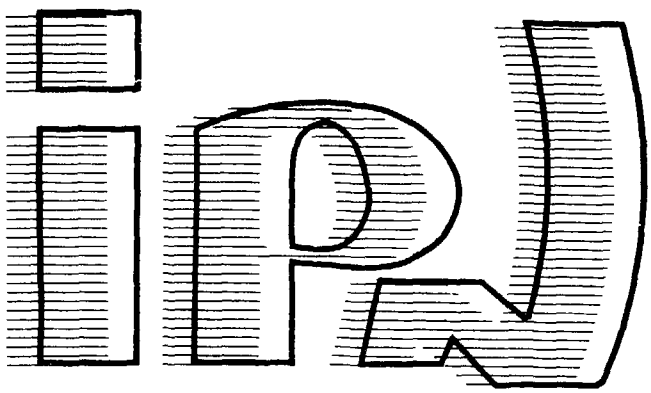

IPNO DRE 93-01

Single-Particle and Collective States in Transfer Reactions

I. Lhenry, T. Suomijärvi
Institut de Physique Nucléaire, CNRS-IN$_2$P$_3$, F91406 Orsay Cedex
Ph. Chomaz
Ganil, BP 5027, F14021 Caen Cedex
Nguyen van Giai
Division de Physique Théorique, Institut de Physique Nucléaire, F 91406 Orsay Cedex

IPNO DRE 93–01

Single-Particle and Collective States in Transfer Reactions

I. Lhenry, T. Suomijärvi
Institut de Physique Nucléaire, CNRS-IN$_2$P$_3$, F91406 Orsay Cedex
Ph. Chomaz
Ganil, BP 5027, F14021 Caen Cedex
Nguyen van Giai
Division de Physique Théorique, Institut de Physique Nucléaire, F 91406 Orsay Cedex

Single-Particle and Collective States in Transfer Reactions

I.Lhenry, T.Suomijärvi
Institut de Physique Nucléaire, CNRS-IN$_2$P$_3$, F-91406 Orsay cedex, France

Ph.Chomaz[1]
Ganil, B.P. 5027, F-14021 Caen cedex, France

and

Nguyen van Giai
Division de Physique Théorique[2]*, Institut de Physique Nucléaire, F-91406 Orsay cedex, France*

January 22, 1993

Abstract:

The possibility to excite collective states in transfer reactions induced by heavy ions is studied. Collective states are described within the Random Phase Approximation (RPA) and the collectivity is defined according to the number of configurations contributing to a given state. The particle transfer is described within the Distorted Wave Born Approximation (DWBA). In the particular case of a one-hole target nucleus, the particle transfer to the nucleus induces particle-hole excitations. These doorway states are then recoupled to eigenstates of the nucleus which are assumed to be RPA states. Calculations are performed for two different stripping reactions: $^{207}Pb(^{20}Ne, ^{19}Ne)^{208}Pb$ and $^{59}Co(^{20}Ne,^{19}F)^{60}Ni$ at 48 MeV/nucleon for which experimental data are available. The calculation shows that even though the transfer spectrum is dominated by non-collective high-spin states due to the matching conditions, a sizable fraction of collective strength can be excited in these reactions. The comparison with experiment shows that this parameter-free calculation qualitatively explains the data.

[1] *On leave from Division de Physique Théorique, Institut de Physique Nucléaire, F-91406 Orsay cedex, France*

[2] Unité de recherche des Universités Paris-XI et Paris-VI, Associée au CNRS

1 Introduction

The availability of intermediate energy heavy-ion beams has prompted the study of the high-excitation energy region in transfer reactions. In several one-nucleon transfer reactions, a broad structure has been observed in the energy spectrum around 10-20 MeV depending on the target nucleus [1, 2, 3]. It has been suggested that these structures are due to the excitation of high-spin single-particle states. The width of the bumps has been explained by the coupling of these states to low-lying collective states [2, 3].

To explain the overall shape of the inclusive one-nucleon transfer spectra, a semi-classical model has been proposed by Bonaccorso and Brink [4]. This model treats the absorption on quasi-bound or unbound states in the target as well as the elastic break-up of the projectile. The observed bumps in transfer spectra are interpreted as being due to the excitation of single-particle resonance states in the target nucleus.

However, the excitation energies of the observed structures roughly vary as $A^{-1/3}$ for different nuclei and correspond approximately to those of the well known giant resonances. Their widths, a few MeV, are also comparable to the giant resonance widths. Furthermore, in several experiments, it has been shown that giant resonances are strongly excited in inelastic heavy ion collisions [5]. These considerations have raised the interesting question of whether the structures seen in the heavy-ion induced transfer reactions could be due to collective particle-hole excitations such as giant resonances. This would be of great interest because nucleon stripping reactions can be considered as the inverse process of the nucleon decay of giant resonances towards the ground state of the A-1 nucleus, and thus one may hope to study the microscopic structure of the resonances and to control the different branching ratios extracted from decay studies.

In several one-nucleon stripping reactions on one-hole target nuclei induced by light ions, evidence for the excitation of collective low-lying 2^+ and 3^- states has been reported [6, 7]. Moreover, a theoretical model based on the quasi-particle approximation including a pairing interaction and a long-range residual interaction predicts non-negligible excitation of low-lying vibrational states in transfer reactions [8].

In this paper we present microscopic calculations for one-nucleon stripping reactions on one-hole target nuclei. This can be viewed as a one-step process where a particle is deposited on the core and then recoupled via the residual interaction to the normal modes of the target. It must be noticed that this process is quite different from the excitation of a particle state plus a phonon in a two-step process. Even if no clear signature of such a two-step process has been experimentally observed, it can contribute to the transfer spectra and still needs to be estimated. The cross section of each excited state given by the RPA is evaluated, by using the RPA amplitudes in a DWBA calculation. The calculations have been done for two different reactions: $^{207}Pb(^{20}Ne,^{19}Ne)^{208}Pb$ and $^{59}Co(^{20}Ne,^{19}F)^{60}Ni$ at

48 MeV/nucleon. The results are compared to experimental spectra measured at GANIL for these two reactions [9].

In these reactions a nucleon is transferred to a non-closed shell target nucleus and thus particle-hole excitations can be created in a one-step process. The angular-momentum matching conditions in heavy-ion reactions favour nucleon transfer to high angular-momentum orbitals. The coupling of this transferred particle with the pre-existing hole state defines the range of multipolarities that can be excited in the final nucleus. In the case of the ^{207}Pb target, the hole state is $3p_{1/2}$ and therefore only high multipolarities in ^{208}Pb are expected. On the other hand, the hole state in ^{59}Co has a rather high spin ($1f_{7/2}$) and thus, low multipole modes should also be excited.

The amount of collective strength that can be excited in the transfer reactions depends on the number of particle-hole configurations and the corresponding transfer cross section. In the case of ^{207}Pb only two different particle states can be coupled to a given total angular momentum. This makes ^{207}Pb target an unfavorable candidate for collective excitations. The high spin of the hole state in ^{59}Co allows a wider range of multipolarities and thus enhances the possibility to excite collective strength. The importance of the particle-hole correlations and collective excitations in the case of the two studied reactions will be discussed.

2 RPA-DWBA Calculations

2.1 Inelastic and Transfer Cross Section

The Random Phase Approximation (RPA) describes giant resonances, $|\nu\rangle$, by a coherent sum of particle-hole excitations:

$$|\nu\rangle = \sum_{ph} \left(X^{\nu}_{ph} a^{+}_{p} a_{h} + Y^{\nu}_{ph} a^{+}_{h} a_{p} \right) |0\rangle \qquad (1)$$

where p (resp. h) labels the particle (resp. hole) states and where $|0\rangle$ is the RPA ground state. In equation (1) X and Y are the solution of the RPA equations [10]. The transition amplitude between the excited state $|\nu\rangle$ and the ground state $|0\rangle$ induced by a one-body operator F is given by :

$$\langle 0|F|\nu\rangle = \sum_{ph} F_{hp} X^{\nu}_{ph} + F_{ph} Y^{\nu}_{ph} \qquad (2)$$

where F_{ph} are the particle-hole matrix elements of the Hermitian operator F. For instance, for inelastic scattering at a given angle θ, one can use the Distorted Wave Born Approximation (DWBA) to compute the particle-hole matrix

elements $A_{ph}(E,\theta)$ so that the final cross section reads :

$$\frac{d\sigma}{d\Omega dE} = \sum_{\nu} |\sum_{ph} A_{hp}(E,\theta)X^{\nu}_{ph} + A_{ph}(E,\theta)Y^{\nu}_{ph}|^2 \delta(E - E_{\nu}) \qquad (3)$$

In a transfer reaction on a non-closed shell nucleus such as ^{207}Pb or ^{59}Co, by adding a particle, a part of the ph-configurations contributing to the giant resonance strength in the final nucleus can be populated. Indeed, the target ground state can be approximated, retaining only the leading order, by a single hole (h_0) excitation on the neighbouring closed-shell ground state:

$$|h_0\rangle = a_{h_0}|0\rangle. \qquad (4)$$

and when a particle is transferred a pure particle-hole state is excited. This approximation corresponds to neglecting all kind of correlations and in particular it corresponds to neglecting the contributions of the Y amplitudes describing the RPA ground-state correlations. In this case the RPA reduces to the Tamm-Dancoff Approximation (TDA). The amplitude $A_p(E,\theta)$ to transfer a particle to a given particle state p during a scattering to an angle θ with an energy loss E can be computed using the DWBA and the cross section can now be estimated by :

$$\frac{d\sigma}{d\Omega dE} = \sum_{\nu} |\sum_{p} A_p(E,\theta)X^{\nu}_{ph_0}|^2 \delta(E - E_{\nu}) \qquad (5)$$

One can notice that the transfer cross section is equivalent to the inelastic cross section except for the very particular excitation operator :

$$A_{ph} = A_p \delta_{h,h_0} \qquad (6)$$

2.2 Schematic Model

By using a simple schematic model, we can show how the cross section of a given RPA state excited in an inelastic scattering can be amplified compared to that of a single p-h state, due to coherent effects. We can also illustrate the fact that, even if the number of p-h configurations of the RPA state involved in the transfer is smaller than in the inelastic reactions, transfer reactions may still present some coherent effects.

Let us consider a schematic model where ν, a collective excited state of a closed-shell nucleus, can be written as the sum of Ω identical p-h configurations having the same energy, wave function and RPA amplitude $X^{\nu}_{ph} = 1/\sqrt{\Omega}$. This is a typical collective state because many configurations contribute to the wave function. The larger the number Ω, the more collective the state is. If this collective state is excited with an appropriate operator, the different p-h configurations can be excited in a coherent way and its transition probability can be much larger

than the elementary one. Indeed, if we consider an operator for which all the different p-h matrix elements are equal, $A_{ph} = Q$, we get a transition probability:

$$P_\nu = |\langle 0|Q|\nu\rangle|^2 = |\sum_{ph} X^\nu_{ph} Q_{ph}|^2 = \Omega Q^2 \tag{7}$$

Here, the transition probability is Ω times the elementary transition probability, $P_{ph} = Q^2$, so that such a state gives rise to a giant response. This is what may happen during an inelastic excitation. Therefore, a collective state can be called giant for a given excitation operator if this operator creates coherence between the different p-h configurations of the state. Then, the notion of "giant", contrarily to the notion of "collective", is bound to the operator. This is in fact a very well known feature, for example the Giant Dipole Resonance appears as a very weak excitation in α-particle scattering in which the external perturbation is isoscalar whereas it is strongly excited in photoabsorption reactions which create an isovector excitation field.

Now, if we consider a transfer reaction where N p-h configurations of the RPA state ν are excited with the same amplitude $A_p = Q$, the excitation probability of this state is given by :

$$P_\nu = |\sum_p X^\nu_{ph_0} A_p|^2 = \frac{N^2}{\Omega} Q^2 \tag{8}$$

This demonstrates that the coherence factor in transfer reaction is N^2/Ω which can be larger than 1 but is always less than Ω. This model shows that the transfer cross section of an RPA state can be much larger than the elementary cross section of a single p-h state, but that this coherent effect will in general be smaller for a transfer reaction than for the inelastic scattering. In the case of ^{208}Pb, only 2 configurations are allowed whereas in the case of ^{60}Ni, 7 configurations can be excited. The approximate value of Ω is about 10 for giant resonances. From this very simple schematic model one can conclude that ^{60}Ni is a good candidate for the excitation of giant states by one-nucleon transfer reactions while ^{208}Pb is less favourable.

This shows that it is theoretically possible to excite a giant state by transferring a nucleon to a non-closed shell target nucleus. The problem is now to know whether, in the considered reactions, the populated states are collective and whether they are excited with enough configurations and with enough coherence to be giant.

3 Results of the Calculation

The self-consistent Hartree-Fock (HF) and discrete RPA calculations were performed using the Skyrme force SGII [11] within a large harmonic oscillator basis. All different transitions to electric multipoles from L=0 to L=9 were

considered. In the case of transfer reactions, the isospin was not taken as a good quantum number so that isoscalar and isovector states are mixed in the response associated with a given spin and parity. As far as the magnetic states are concerned, only a non-interacting p-h model has been used because they are generally weakly perturbed by the inclusion of the residual interaction. The HF basis was taken large enough in order to have 100% of the Energy Weighted Sum Rule (EWSR) even for high multipolarities. In the following, each RPA-state is graphically represented by a gaussian distribution with a FWHM of 0.5 MeV.

3.1 Definition of Collectivity

The aim of this paper is to study to what extent it is possible to excite collective states in transfer reactions. It is thus very important to first establish criteria defining collective states. This can be done by analysing the strength distributions obtained in inelastic scattering. Giant resonances are a typical example of collective states. Their strength is generally several single-particle units (s.p.u.) due to a coherent sum of several p-h configurations. Furthermore, the effect of the residual interaction is important in producing shifts and mixing of simple p-h configurations. Thus, a comparison between RPA and HF calculations together with the strength allows to select collective states. However, this selection is not exhaustive because some collective states may not be strongly excited by the considered operator.

In Fig. 1.a, the RPA strength (shaded area) in s.p.u. for ^{208}Pb is compared to the strength obtained with no residual interaction (solid line) for the natural parity isoscalar transition of L=2,4 and 6. In the case of L=2, a very strong effect of the residual interaction is observed. In the RPA calculation the strength is shifted to lower excitation energies and is essentially concentrated into two states at 5.6 MeV and 11.6 MeV. The first peak corresponds to the first low lying 2^+ state in ^{208}Pb which is experimentally observed at 4.1 MeV and the second one corresponds to the Isoscalar Giant Quadrupole Resonance (ISGQR). The strength of these states is several s.p.u. Taking into account previous observations, these two states can clearly be called collective. In the same way, in the case of L=4, collective states are observed at 6.0, 8.5, 12.3 and 12.7 MeV. For high multipolarities, the transition strength decreases and the effect of the residual interaction becomes less important. In the case of L=6, both HF and RPA strength distributions are spread out with a maximum value of only 3 s.p.u.

It is useful to define a criterium for a collective state in terms of the number of configurations in a given RPA state and of a maximum weight of each p-h configuration. The number of configurations is defined to be the minimum number of p-h states required to exhaust more than 95% of the total normalisation of the state. These criteria can then be easily defined requiring that all giant states must be collective. From the previous discussion on the giant states, the following condition for collective excitation can be adopted. In the case of ^{208}Pb, a

state is defined as collective if at least 5 p-h configurations contribute to the wave function with a relative weigth X^2 less than 0.85. Fig.1.b shows the collective strength (black area) obtained for isoscalar states L=2, 4 and 6 in ^{208}Pb using the above definition. It is interesting to notice that the amount of collective strength clearly decreases for high multipolarities.

Fig. 2.a shows a comparison of strength distributions obtained by RPA (shaded area) and HF (solid line) calculations for isoscalar states L=2, 4 and 6 in ^{60}Ni. By using the same considerations as for ^{208}Pb, collective states are observed at 2.0, 16.1 and 17.5 MeV in the case of L=2, the peaks at 16.1 and 17.5 MeV corresponding to the ISGQR, and at 16.8 MeV in the case of L=4. This leads to the following condition for a collective state in ^{60}Ni: it has at least 3 configurations with a relative weight less than 0.9. Fig. 2.b shows the collective strength such defined in the case of ^{60}Ni. It should be noted that the number of configurations needed for collective states is lower than in the case of ^{208}Pb. In fact, in the case of light nuclei, the number of holes is smaller and thus the number of particle-hole configurations available for collective states is also smaller. This leads also to a weaker strength for these states as can be seen in Fig. 2.

3.2 Cross Section Calculation for Transfer Reactions

The calculation of transfer cross sections was done by using eq. 5 for the following reactions: $^{207}Pb(^{20}Ne,^{19}Ne)^{208}Pb$ and $^{59}Co(^{20}Ne,^{19}F)^{60}Ni$. The DWBA cross sections were calculated by the code PTOLEMY [14]. This code was adapted to calculate transfer to unbound states by using the same particle wave functions used in the discrete RPA calculations. All different transitions to bound and quasi-bound target states were considered. Quasi-bound states were defined as states whose energy is practically independent of the boundary condition in the HF calculation. This limits the maximum excitation energy to 18 MeV for ^{208}Pb and to 25 MeV for ^{60}Ni. The contributions of three different final states $2s_{1/2}$, $1p_{1/2}$ and $1d_{5/2}$ of ^{19}Ne and ^{19}F were considered with respective weights C^2S given by spectroscopic factors from the calculation of ref. [15]: 0.56 ,1.97 and 1.03 respectively. This calculation gives the same spectroscopic factors for both nuclei since they are described as mirror nuclei. The optical parameters were obtained from references [5] and [13]. It should be noted that this calculation has no free parameters.

Figs. 3 and 4 show for ^{208}Pb and ^{60}Ni, respectively, the total cross section of each multipolarity for different final hole states of the ejectile and for the sum of these states. These two figures illustrate the angular momentum matching conditions which can be understood as follows: by using a very simple hypothesis where a nucleon is transferred to the surface of a nucleus at rest, the transferred angular momentum ΔL can be estimated as ΔL = Rp, where R is the radius of the target and p the nucleon linear momentum. For the ^{20}Ne projectile at 48 MeV/nucleon this gives $\Delta L \approx 7$ for the ^{60}Ni target and $\Delta L \approx 11$ for the ^{208}Pb target. It should be noted that this gives only a very simplified picture

of transfer reactions in which generally rather complicated selection rules and matching conditions are involved (ref. [16]).

In the case of ^{208}Pb, the effect of the final target state is clearly seen in the case of $d_{5/2}$ and $s_{1/2}$, although it is less evident for $p_{1/2}$ (Fig.3). For ^{60}Ni the preferential angular momentum is lower than for ^{208}Pb. Moreover, the proton hole state in ^{59}Co has an angular momentum $f_{7/2}$ and the coupling to the final state gives different multipolarities from $J_B = L_f - 3$ to $L_f + 3$. Thus in the case of ^{60}Ni also low multipole modes can be reached contrarily to ^{208}Pb. This is clearly seen in the cross-section distributions (Fig. 4) which are flatter than in the case of ^{208}Pb. However, this effect is attenuated due to the spin factor $2J_B+1$ which increases the high multipolarity cross sections.

3.3 Effects of Collectivity

In the following, we will discuss the effect of the residual interaction and the importance of collective excitations in transfer reactions. For a collective state, the criteria defined in subsection 3.1 will be used.

The transfer cross section for ^{208}Pb is presented in Fig. 5. Fig. 5.a shows the difference between the RPA (shaded area) and HF (solid line) calculation. A small effect due to the residual interaction can be seen at 5 MeV and at about 14 MeV. At 5 MeV the cross section corresponds to the excitation of the $(g_{9/2}, p^{-1}_{1/2})$ component of the 5^- state. At about 14 MeV the effect of the residual interaction is observed in 9^-, 6^+ and 4^+ multipole states. In Fig 5.b, the contribution of collective states is indicated by black areas. A non-negligible amount of cross section is observed to be due to collective excitations at about 14 MeV corresponding to 4^+ and 6^+ multipole states. At 5 MeV, where the effects of the residual interaction were found to be important, only a small amount of collective strength can be seen. In fact, a strong effect due to the particle-hole interaction is a necessary but not a sufficient condition to observe a collective excitation.

In the case of ^{60}Ni, the residual interaction is important leading to a spreading of the cross section as can be seen in Fig. 6.a. In Fig. 6.b, a collective component is observed at 7 MeV corresponding to L=4 multipolarity. At higher excitation energies an important cross section for collective excitations is found at about 20 MeV. This corresponds to excitation of L=3, 4, 5 and 6 multipolarities. In fact, in the case of L=3 and 4, nearly the total cross section obtained for stripping reaction is due to collective excitations.

In order to get a deeper insight in the effects of the residual interaction and of coherence in transfer reactions, we will discuss in more detail the L=2 and L=3 multipole states in ^{60}Ni. In the case of L=2, an increase of the cross section is observed at about 7 MeV (Fig. 7.a, shaded area). This is due to a coherent sum of only two particle-hole configurations and thus using the previously defined criteria, the corresponding RPA-state is not collective, as can be seen in Fig.7.b. On this figure one clearly observes the contribution of the ISGQR which corresponds

to the two peaks around 16MeV and 17.5MeV. However these states are weakly populated by this transfer reaction. For L=3, the effect of residual interaction is very important (see Fig. 8.a) and many collective states are excited such as the low lying 3^- state (see Fig. 8.b). However, we mainly observe a spreading of the strength with no global increase of the cross section.

These considerations show clearly that both conditions of collectivity and coherence are necessary in order to excite giant states.

4 Comparison of Experimental and Calculated Transfer Cross Sections

In this section we compare the theoretical predictions and the experimental data taken at the GANIL national facility in France [9].

4.1 $^{207}Pb(^{20}Ne,^{19}Ne)^{208}Pb$

Fig. 9.a presents a spectrum measured for the reaction $^{207}Pb(^{20}Ne,^{19}Ne)^{208}Pb$ [9]. The calculated transfer cross section integrated over the experimental angular range of 5.0°-9.0° in the center-of-mass frame, is plotted in Fig. 9b. It is noted that a smooth background due to break-up reactions is superimposed to the experimental spectrum. In order to compare experimental and calculated cross-section values, the contribution of non-natural parity states has been included in the calculated spectrum. In the calculation,the residual interaction for the non-natural parity states was assumed to be negligible.

In the experimental spectrum of Fig. 9.a, the first excited state is observed at 3 MeV corresponding to the excitation of $(g_{9/2}, p^{-1}_{1/2})$. The $(g_{7/2}, p^{-1}_{1/2})$ component of the collective 3^- state observed in (p,d) reaction at 2.6 MeV (ref. [17]) is not excited in the $(^{20}Ne,^{19}Ne)$ reaction. This is due to the high angular momentum matching condition with ^{20}Ne projectiles. For the same reason, the transfer to $i_{11/2}$ and $j_{15/2}$ has a larger cross section than transfer to the $d_{5/2}$ orbital which in (d,p) reaction is strongly excited at 5.0 MeV. The calculation is in agreement with observed relative intensities for low-lying states.

In the experimental spectrum, at about 13.5 MeV a large bump is observed superimposed on a continuum which is partly due to the projectile breakup process. The calculation gives a strong concentration of cross section between 12 and 17 MeV corresponding to the bump in the experimental spectrum. The cross section in this excitation energy region is due to the excitation of high multipolarities ($L > 6$) corresponding to the following particle-hole configurations: $(k_{17/2}, p^{-1}_{1/2})$, $(i_{13/2}, p^{-1}_{1/2})$, $(j_{13/2}, p^{-1}_{1/2})$ and $(h_{11/2}, p^{-1}_{1/2})$. Part of the cross section is coming from

collective states but their contribution is not dominant. These collective excitations are associated with high multipolarities and therefore, transfer reactions may be a way to study high L resonances if one is able to extract them from the background. In the case of ^{208}Pb, the calculated spectrum is in rather good agreement with the experimental one in the excitation energy domain covered by the calculation. The absolute cross section is comparable to the experimental one. The excitation of low multipole modes is unfavoured and thus the low-lying 2^+ and 3^- states are observed neither in the calculation, nor in the experimental data.

The low-lying states appear as peaks both in the experimental and theoretical spectra. Conversely, the high-lying states are observed as a broad structure in the data. This is due to the fact that at these excitation energies a state has a small life time due to a large number of open decay channels. This gives a width of several MeV to all the states in this region. Taking into account this width in the theoretical prediction would bring it very close to the experimental observation. It should be noted that similar spectra were measured for a ^{207}Pb target in a recent experiment performed at MSU using slightly different beams ([18]).

4.2 $^{59}Co(^{20}Ne,^{19}F)^{60}Ni$

Fig. 10.a presents an experimental spectrum for the $^{59}Co(^{20}Ne,^{19}F)^{60}Ni$ reaction [9]. In this case, the absolute normalisation was not possible due to experimental problems and the spectrum is thus presented in counts. The calculated cross section is presented in Fig. 10.b. In this reaction, the ground state is only weakly excited. At about 1.3 MeV a small peak corresponding to the $(p_{3/2}, f_{7/2}^{-1})$ component of the collective 2^+ state is observed. In the (α,t) reaction of ref. [19] the first 2^+ state is strongly excited. The collective 3^- state in ^{60}Ni is located at 4 MeV. Some evidence of excitation of this state in (α,t) reaction is reported in ref. [19]. Unfortunately, in the $(^{20}Ne,^{19}F)$ spectrum this state is not resolved from the $(f_{5/2}, f_{7/2}^{-1})$ state at 5 MeV.

The peak at 6.4 MeV has no clear assignment but could also be due to the $(f_{5/2}, f_{7/2}^{-1})$ or to the $(g_{9/2}, f_{7/2}^{-1})$ excitation.

The calculation predicts a very strong excitation of the $(f_{5/2}, f_{7/2}^{-1})$ configuration while the low-lying 3^- and 2^+ states are only weakly excited. It should be noted also that the $(f_{5/2}, f_{7/2}^{-1})$ is fragmented into two components. At about 11 MeV a pronounced peak can be seen in the calculated spectrum. This is due to the transfer to $g_{9/2}$ orbital. In the experimental spectrum, a large bump is observed at this excitation energy but with a much weaker relative intensity.

Between 17 MeV and 22 MeV, two rather fragmented peaks are observed in the calculation. In this excitation energy region, the largest cross section is due to multipolarities $L > 5$ corresponding to $(h_{11/2}, f_{7/2}^{-1})$, $(f_{7/2}, f_{7/2}^{-1})$ and $(g_{7/2}, f_{7/2}^{-1})$

configurations. However, part of this strength is collective. This component is not really observed in the experimental spectrum except as a wide shoulder above the break-up background. This may be due to the decay width of the states which when added to the predicted spreading of the high energy strength would wash out the concentration of strength around 20 MeV.

In the case of ^{60}Ni, the agreement with the experimental spectrum is only qualitative. In particular, the first 2^+ state is clearly observed in the experimental spectrum while the calculation gives only a very small cross section because of the strong matching conditions .

5 Conclusion

In this paper we have presented a microscopic calculation coupling the RPA strength function and the DWBA cross section for stripping reactions on non-closed shell target nuclei. Two reactions have been studied: $^{207}Pb(^{20}Ne,^{19}Ne)^{208}Pb$ and $^{59}Co(^{20}Ne,^{19}F)^{60}Ni$ at 48 MeV/nucleon.

Due to the high angular-momentum matching condition only high-multipolarity states are excited in ^{208}Pb. In the case of ^{60}Ni, high multipolarity states are not as dominant as in the case of ^{208}Pb because of the high spin of the ^{59}Co target nucleus.

We have shown in this paper that the residual interaction is important in stripping reactions on non-closed shell target nuclei also at high excitation energies. However, particle-hole correlations disappear for high multipolarities and thus the effect is more important for the ^{59}Co target than for the ^{207}Pb target.

To conclude, we have seen that in the studied transfer reactions, it is possible to excite collective strength. However, collective states are mostly predicted and observed in low multipole modes which are not dominant in these transfer reactions due to the matching conditions. Moreover, the giant effects, i.e., the increase of the strength due to the coherent summation of particle-hole configurations are weak in both reactions. Therefore, one would need to use selective coincidence experiments in order to extract collective states from the background. Moreover, by using reactions for which low-spin transfers are favoured, one could study low-multipole giant states in transfer reactions.

Acknowledgements

We would like to thank all the experimental group of ref. [9] for allowing us to use their results prior to publication, and also Françoise Samaran for her great help in carrying out the calculations.

References

[1] Ph. Chomaz, N. Frascaria, S. Fortier, S. Galès, J. P. Garron, H. Laurent, I. Lhenry, J. C. Roynette, J. A. Scarpaci, T. Suomijärvi, N. Alamanos, A. Gillibert, G. Crawley, J. Finck, G. Yoo and A. Van der Woude, Annual Report, IPN-Orsay (1990).

[2] S. Fortier, S. Galès, Sam M. Austin, W. Benenson, G. M. Crawley, C. Djalali J. S. Winfield and G. Yoo, Phys.Rev. C41 (1990) 2689.

[3] S. Galès, Ch. Stoyanov and A. I. Vdovin, Phys.Rep. 166 (1988) 125.

[4] A. Bonaccorso and D. Brink, Phys.Rev. C44 (1991) 1559.

[5] T. Suomijärvi, D. Beaumel, Y. Blumenfeld, Ph. Chomaz, N. Frascaria, J. P Garron, J. C. Jacmart, J. C. Roynette, J. Barrette, B. Berthier, B. Fernandez, J. Gastebois, P. Roussel-Chomaz, W. Mittig, L. Kraus and I. Linck, Nucl.Phys. A491 (1989) 314.

[6] NDS, 47 (1986) 840.

[7] NDS, 48 (1986) 340.

[8] Shiro Yoshida, Nucl. Phys. 38 (1962) 380.

[9] I. Lhenry, PhD Thesis, Université d'Orsay (IPNO - T 9201); I. Lhenry, T. Suomijärvi, Y. Blumenfeld, Ph. Chomaz, N. Frascaria, J. P. Garron, J. C. Roynette, J. A. Scarpaci, D. Beaumel, S. Fortier, S. Galès, H. Laurent, A. Gillibert, G. Crawley, J. Finck, G. Yoo and J. Barreto, IV Int. Conf. on Nucl. Nucl. Coll. Kanazawa (Japan), (June 1991).

[10] P. Ring and P. Schuck, "The Nuclear Many-Body Problem", Springer-Verlag, New-York, 1981 and refs. therein.

[11] N. Van Giai and H. Sagawa, Nucl. Phys. A371 (1981) 1.

[12] A. Van der Woude, Prog. Part. Nucl. Phys. 18 (1987) 217.

[13] R. Liguori-Neto, P. Roussel-Chomaz, R. Rochais, N. Alamanos, F. Auger, B. Fernandez, J. Gastebois, A. Gillibert, R. Lacey, A. Miczaika, D. Pierroutsakou, J. Barrette, S.K. Mark, R. Turgotte, Y. Blumenfeld, N. Frascaria, J.P. Garron, J.C. Roynette, J.A. Scarpaci, T. Suomijärvi, A. van der Woude and A. van den Berg, DAPNIA/SPhN 92 23 (1992), to be published in Nucl. Phys. A.

[14] M.H. Macfarlane and S.C. Pieper, ANL Report ANL-76-11 (1976).

[15] T. Engeland and P. J. Elis, Nucl. Phys. A181 (1972) 368.

[16] W. Von Oertzen, Phys.Lett. B151 (1985) 95.

[17] P. B. Vold, J. O. Andreassen, J. R. Lien, A. Graue, E. R. Cosman, W. Dünnweber, D. Schmitt and F. Nüsslin, Nucl. Phys. A215 (1973) 61.

[18] G.H. Yoo, G.M. Crawley, N. Orr, J.S. Winfield, J.E. Finck, S. Galès, Ph. Chomaz, I. Lhenry and T. Suomijärvi , to be published in Phys. Rev. C.

[19] Masaru Matoba, Isao Kumabe and Eiichi Takasaki, Nucl. Phys. A176 (1971) 178.

Figure 1: Strength Function of ^{208}Pb

Strength function in single particle units for ^{208}Pb for the natural isoscalar transition of L=2,4 and 6. Part a. : Comparison between the RPA strength (shaded area) and the one obtained at the HF level (solid line). Part b. : Decomposition of RPA strength (solid line) into collective (black area) and non-collective components.

Figure 2: Strength Function of ^{60}Ni

Same as Fig. 1 for the ^{60}Ni nucleus.

Figure 3: Total Transfer Cross Section for ^{208}Pb

Total transfer cross section to ^{208}Pb as a function of the multipolarity for different final states of the projectile and for the sum over these states.

Figure 4: Total transfer Cross Section for ^{60}Ni

Same as Fig. 3 for the ^{60}Ni nucleus.

Figure 5: Differential Transfer Cross Section for ^{208}Pb

The differential transfer cross section $d\sigma/dE$ is displayed with the same convention as in fig. (1).

Figure 6: Differential Transfer Cross Section for ^{60}Ni

Same as fig. 5 for the ^{60}Ni nucleus.

Figure 7: Differential Transfer Cross Section for quadrupole excitation in ^{60}Ni

Same as fig. 6 for the quadrupole excitations ^{60}Ni nucleus.

Figure 8: Differential Transfer Cross Section for octupole excitation in ^{60}Ni

Same as fig. 6 for the octupole excitations ^{60}Ni nucleus.

Figure 9: Differential Transfer Cross Section for ^{208}Pb

The upper part (a) presents the experimental transfer cross section of the reaction $^{207}Pb(^{20}Ne,^{19}Ne)^{208}Pb$ whereas the lower part(b) displays the predicted cross section. On the theoretical spectrum the collective strength is represented by the black area. The cross sections are integrated over the experimental angular domain $5.0° < \Theta_{CM} < 9.0°$.

Figure 10: Differential Transfer Cross Section for ^{60}Ni

Same as fig. 9 for the $^{59}Co(^{20}Ne,^{19}F)^{60}Ni$ reaction. The cross sections are integrated over the experimental angular domain $2.0° < \Theta_{CM} < 6.0°$.

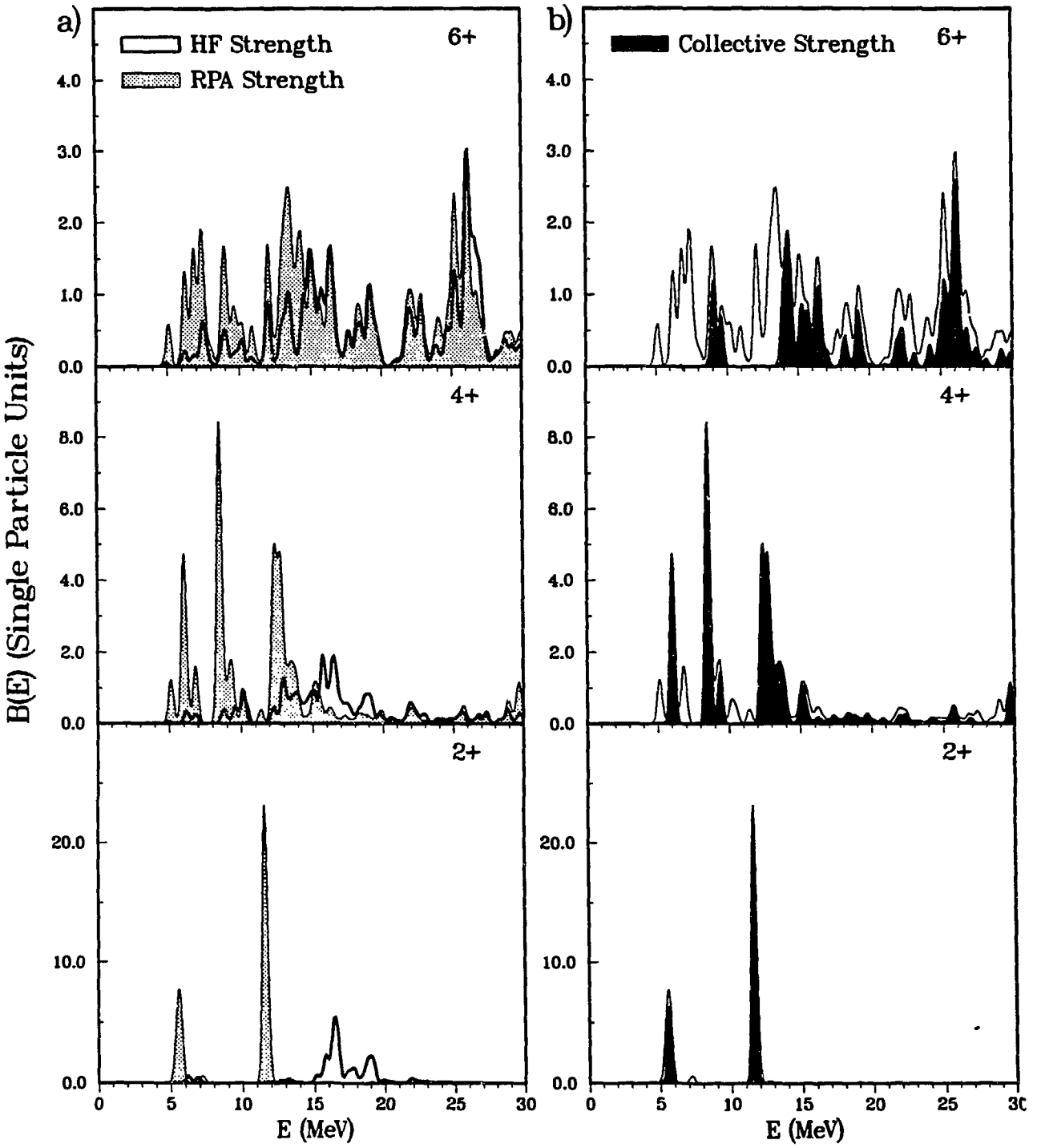
Strength Function for ^{208}Pb
a)
HF Strength
RPA Strength
6+
4+
2+
b)
Collective Strength
6+
4+
2+
B(E) (Single Particle Units)
E (MeV)
E (MeV)

Fig. 1

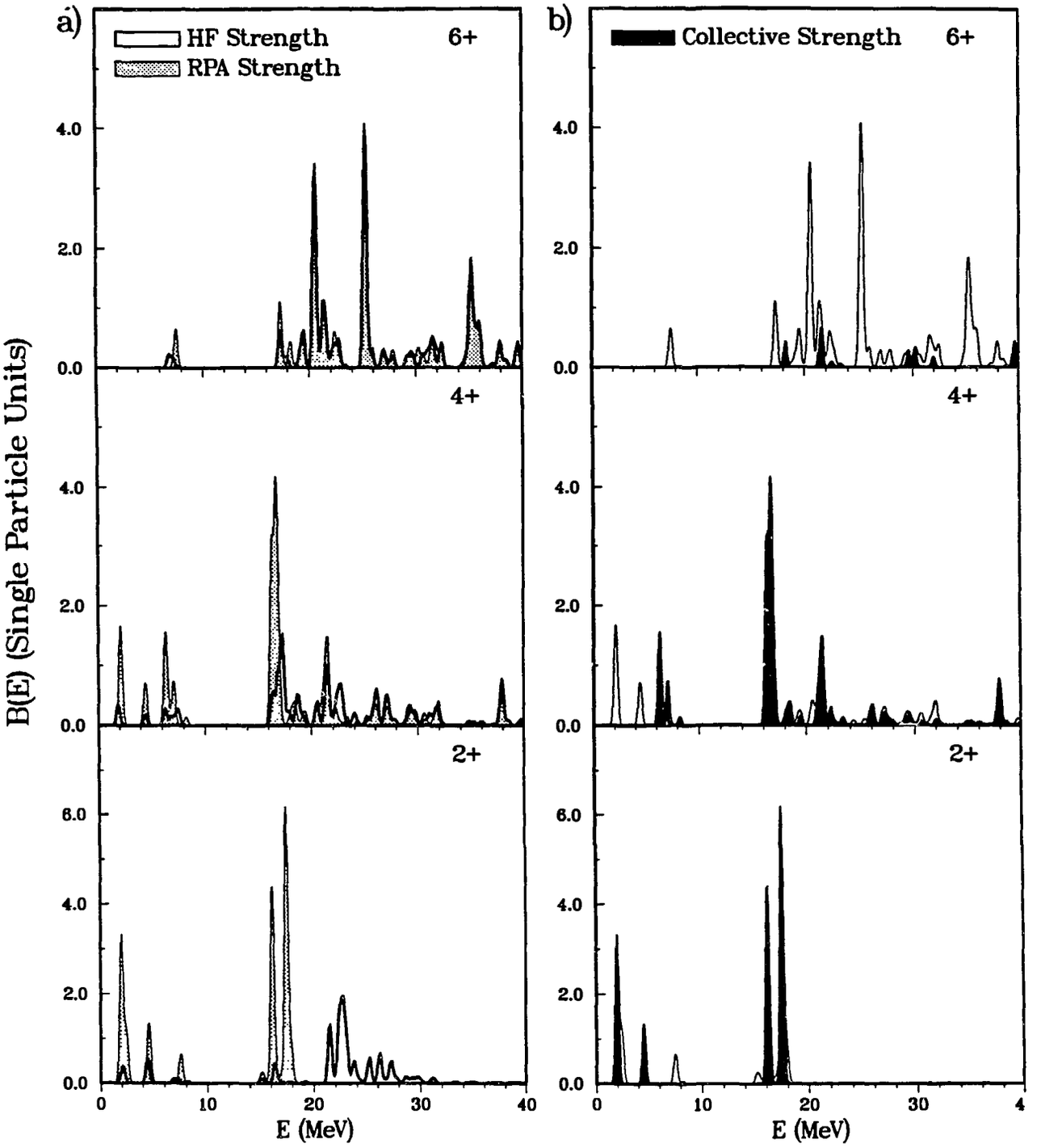
Strength Function for ^{60}Ni
a)
HF Strength
RPA Strength
6+
4+
2+
b)
Collective Strength
6+
4+
2+
B(E) (Single Particle Units)
E (MeV)
E (MeV)

Fig. 2

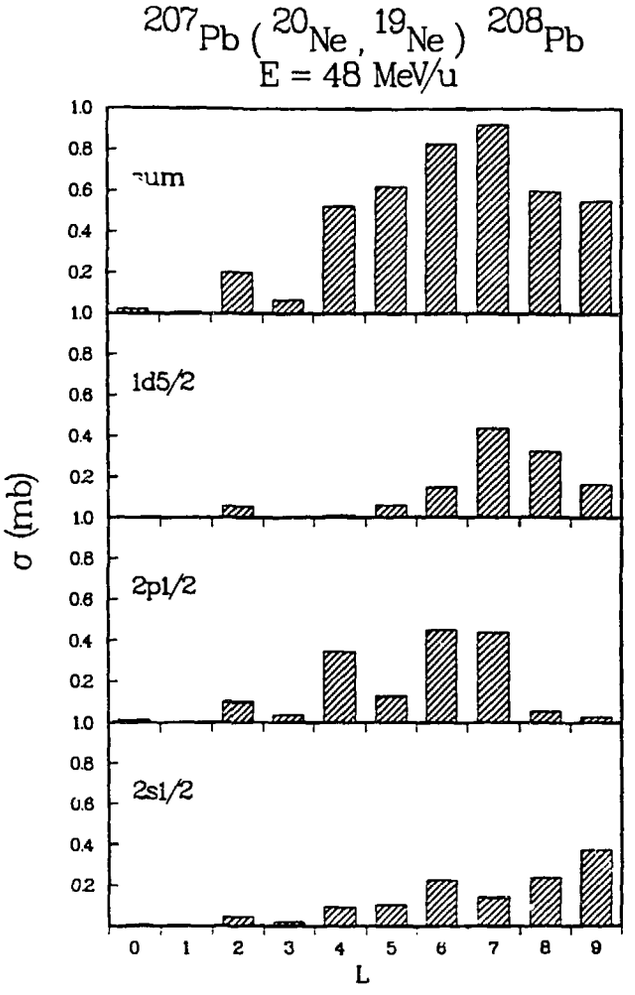

Fig. 3

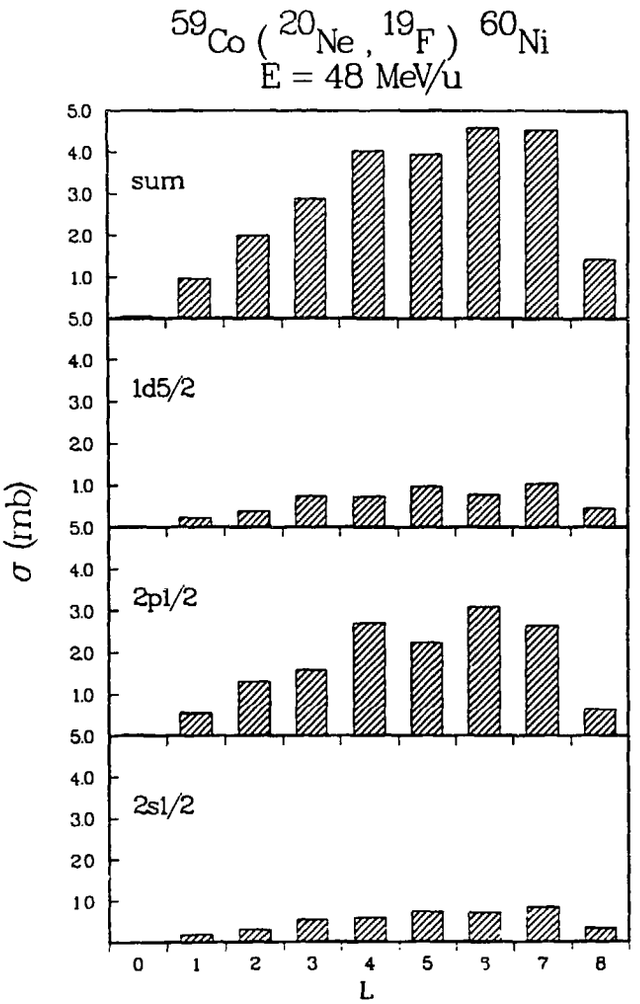

Fig. 4

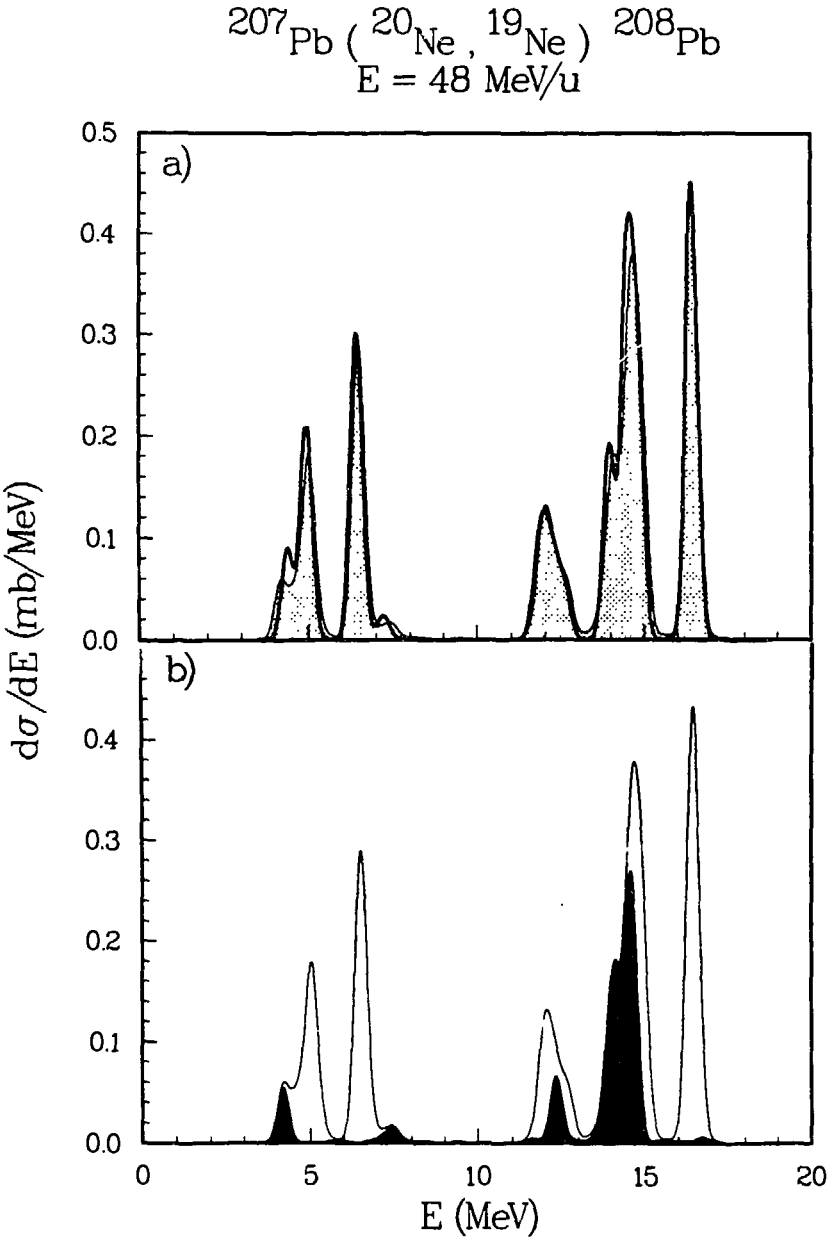
^{207}Pb (^{20}Ne , ^{19}Ne) ^{208}Pb
E = 48 MeV/u
a)
b)
dσ/dE (mb/MeV)
E (MeV)
0.0
0.1
0.2
0.3
0.4
0.5
0
5
10
15
20

Fig. 5

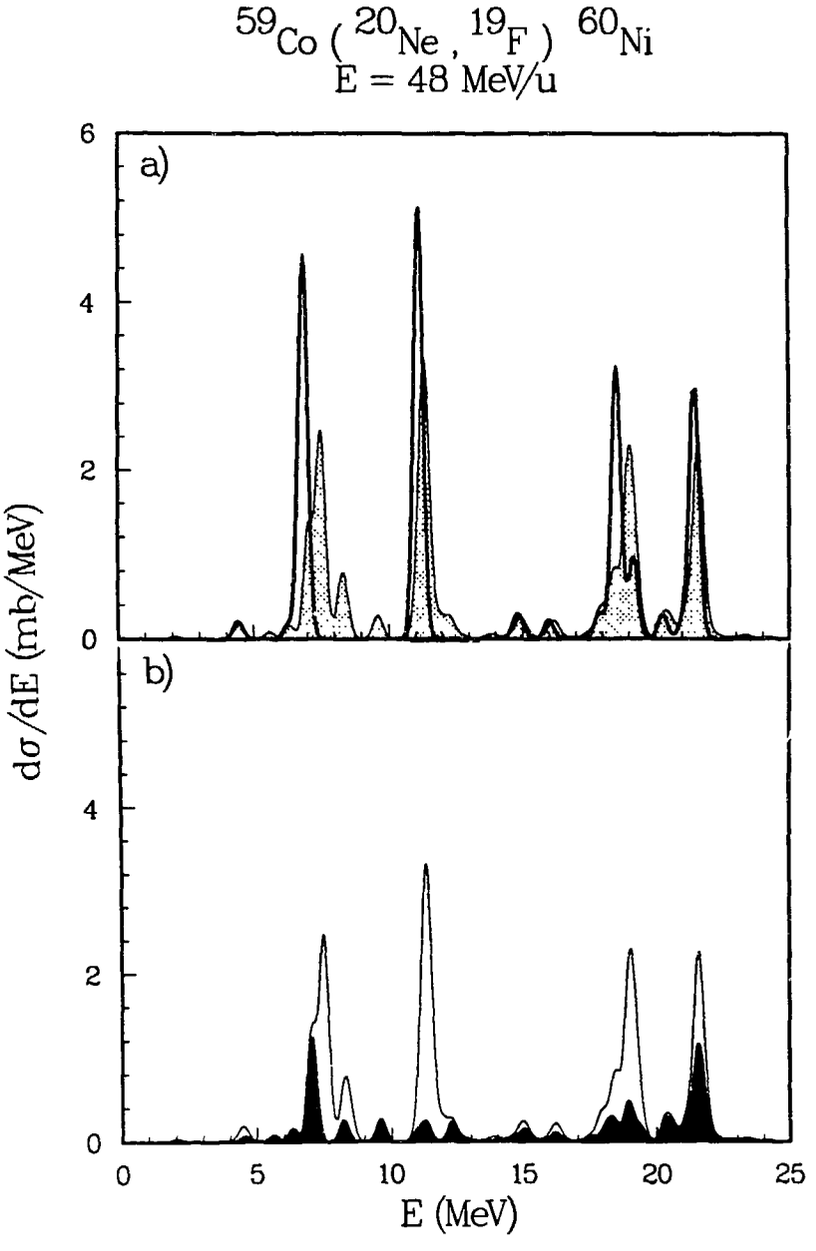
^{59}Co (^{20}Ne , ^{19}F) ^{60}Ni
E = 48 MeV/u
a)
b)
dσ/dE (mb/MeV)
E (MeV)
0
2
4
6
0
5
10
15
20
25

Fig. 6

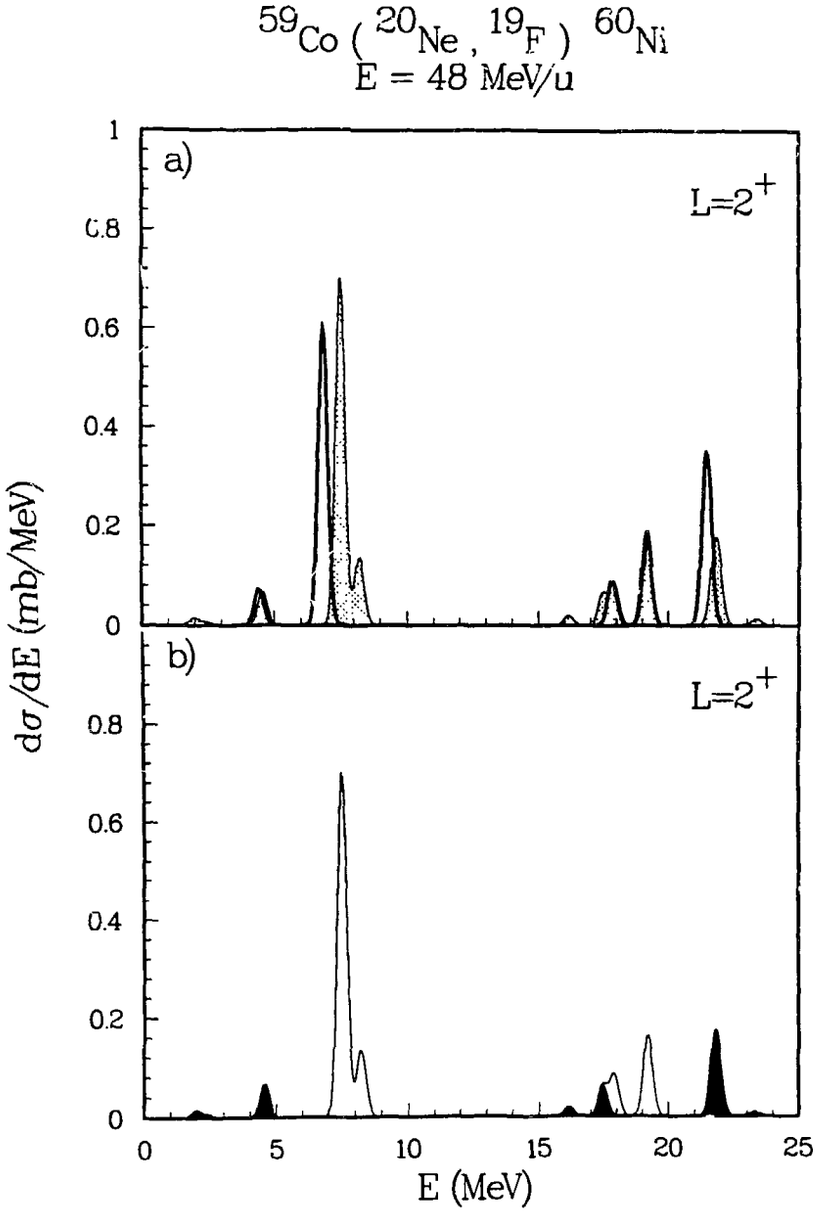
59Co (20Ne , 19F) 60Ni
E = 48 MeV/u
a)
L=2+
b)
L=2+
dσ/dE (mb/MeV)
E (MeV)
0
0.2
0.4
0.6
0.8
1
0
5
10
15
20
25

Fig. 7

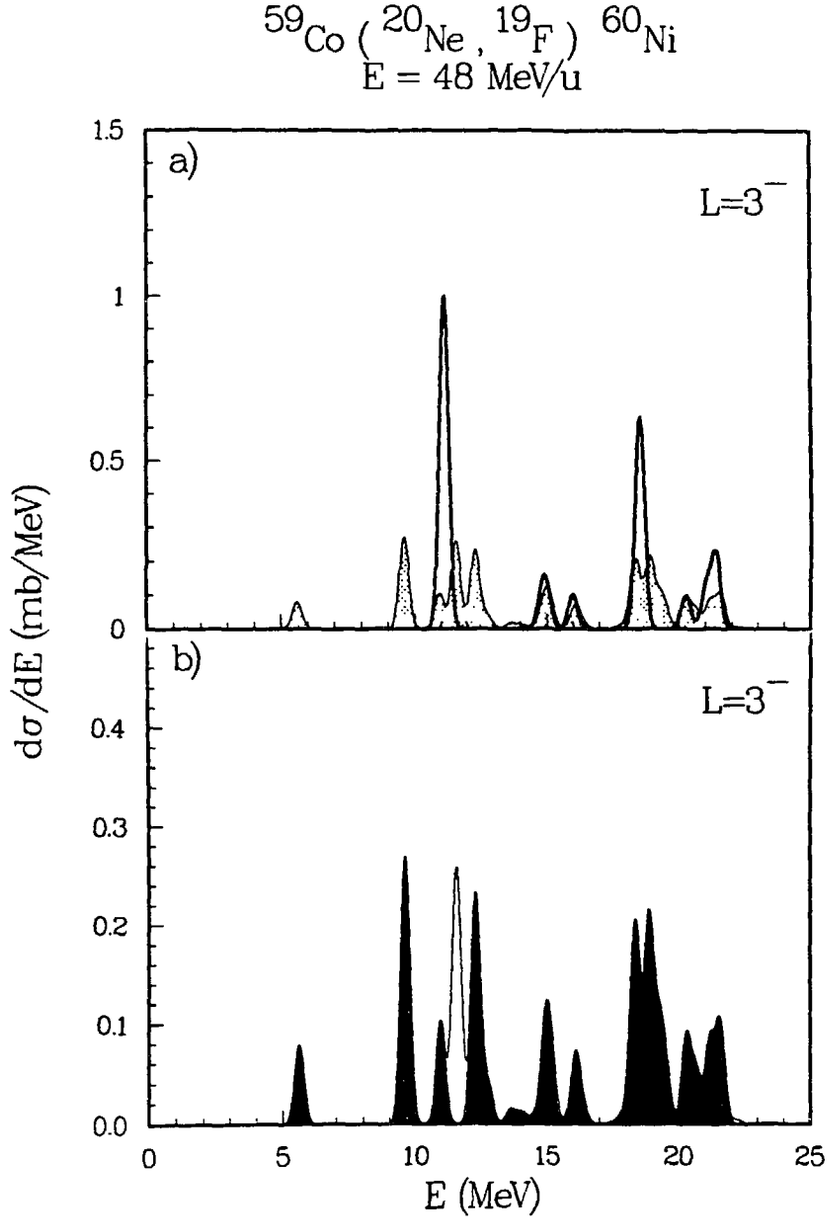
59Co (20Ne , 19F) 60Ni
E = 48 MeV/u
a)
L=3⁻
b)
L=3⁻
dσ/dE (mb/MeV)
E (MeV)
1.5
1
0.5
0
0.4
0.3
0.2
0.1
0.0
0
5
10
15
20
25

Fig. 8

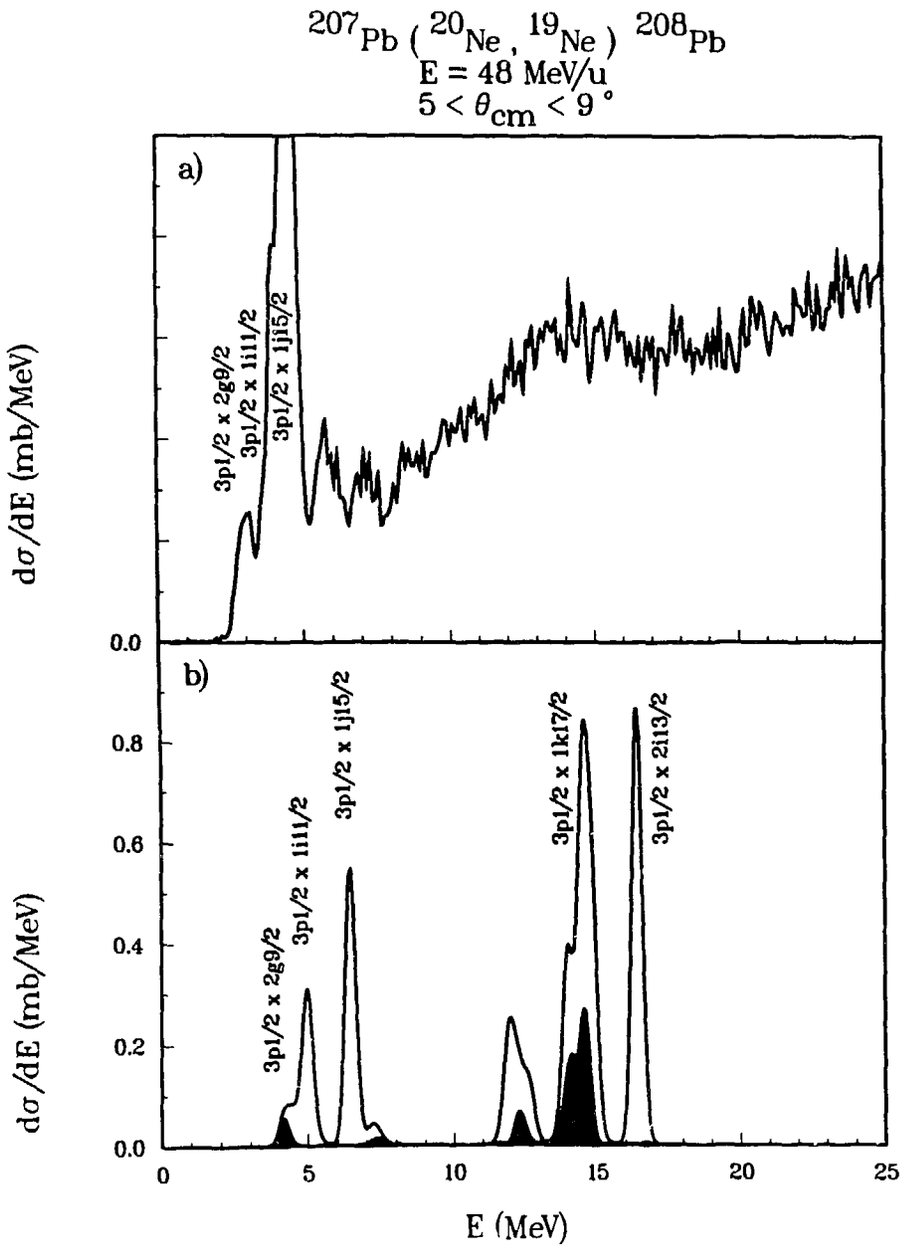
^{207}Pb (^{20}Ne , ^{19}Ne) ^{208}Pb
E = 48 MeV/u
5 < θ_{cm} < 9 °
a)
3p1/2 x 2g9/2
3p1/2 x 1i11/2
3p1/2 x 1j15/2
b)
3p1/2 x 2g9/2
3p1/2 x 1i11/2
3p1/2 x 1j15/2
3p1/2 x 1k17/2
3p1/2 x 2i13/2
dσ/dE (mb/MeV)
dσ/dE (mb/MeV)
0.0
0.2
0.4
0.6
0.8
0
5
10
15
20
25
E (MeV)

Fig. 9

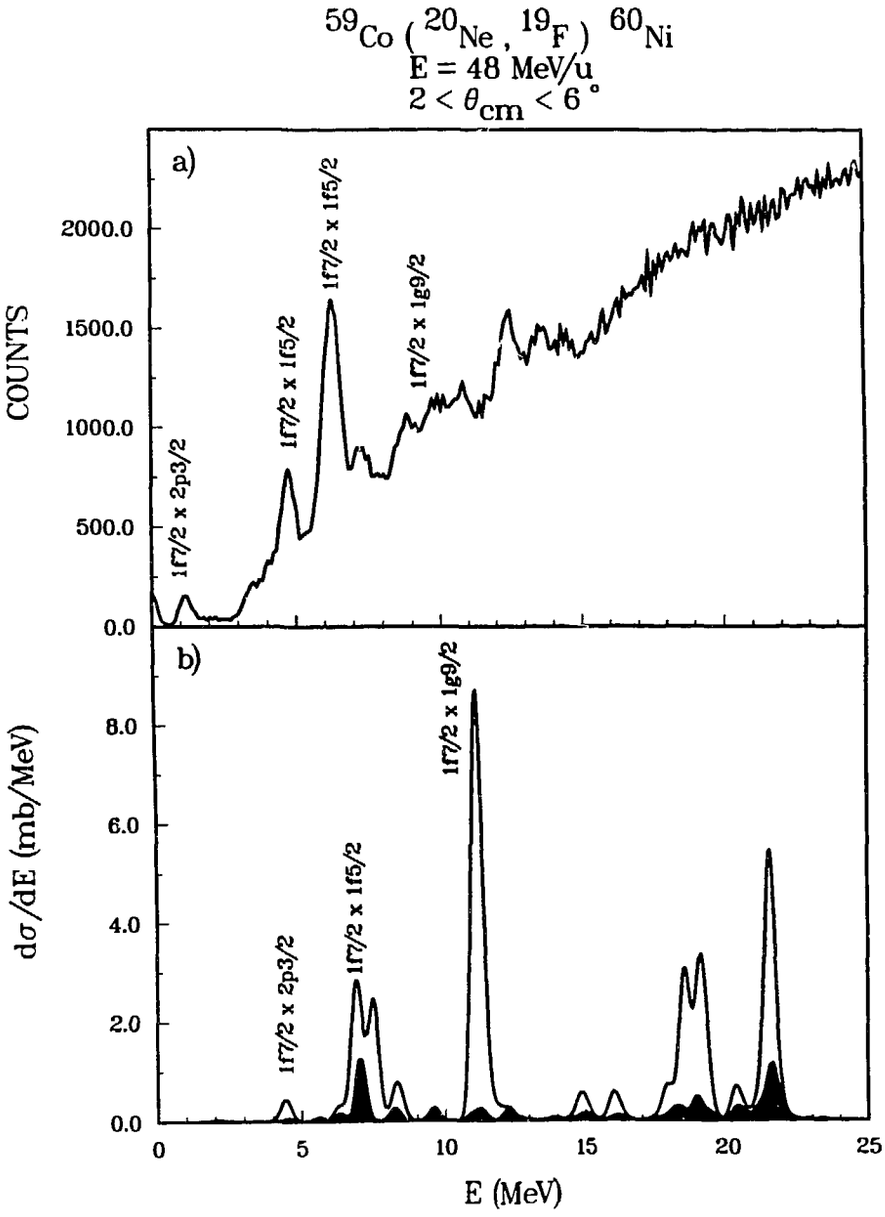
59Co (20Ne , 19F) 60Ni
E = 48 MeV/u
2 < θcm < 6 °
a)
b)
COUNTS
dσ/dE (mb/MeV)
E (MeV)
1f7/2 x 2p3/2
1f7/2 x 1f5/2
1f7/2 x 1g9/2
2000.0
1500.0
1000.0
500.0
0.0
8.0
6.0
4.0
2.0
0.0
0
5
10
15
20
25

Fig. 10